

Structures of RNA Switches: Insight into Molecular Recognition and Tertiary Structure

Harald Schwalbe,* Janina Buck, Boris Fürtig, Jonas Noeske, and Jens Wöhnert*

Keywords:

gene regulation · NMR spectroscopy · RNA · RNA switches · X-ray crystallography

RNA switches (riboswitches) have important functions in gene regulation. They comprise an aptamer domain, which is responsible for ligand binding, and an expression platform that transmits the ligand-binding state of the aptamer domain through a conformational change. Riboswitches can regulate gene expression either at the level of transcription or translation, and it has been proposed that riboswitch mechanisms are even used to regulate the processing of mRNA. This Minireview summarizes the current understanding of the structures and mode of action of RNA switches, with particular focus on secondary and tertiary interactions, which stabilize the global RNA structure and thus determine the function of the aptamer domain.

1. Natural and Non-Natural RNA Aptamers

It has been known for some time that aptamers, that is, RNAs derived from selection procedures (SELEX: selection of ligands by exponential amplification), can bind to a large variety of small-molecule ligands with high selectivity and affinity.^[1] Aptamers bind to ligands^[2] as diverse as nucleotides, amino acids, aromatic dye molecules, coenzymes such as flavinmononucleotide (FMN), aminoglycosides, and S-adenosylmethionine (SAM).^[3] They stem from a randomized starting pool of RNA molecules that typically comprises 10^{14} – 10^{16} mutants. In general, SELEX-derived aptamers bind their small-molecule ligands with affinities in the micromolar

range. Structural analysis of many of the aptamer–ligand complexes show that aptamers form intricate binding pockets for their ligands involving numerous noncanonical RNA structural elements. The interactions include electrostatic and hydrophobic

as well as hydrogen-bonding interactions. In the free form of the aptamer, however, the ligand-binding region is often completely unstructured and ligand binding is accompanied by an induced fit mechanism.

The recent discovery of naturally occurring RNAs, known as RNA switches (riboswitches), that are capable of binding to small-molecule ligands came as a surprise.^[4] The binding of small-molecule ligands to RNA switches is coupled to a novel type of gene expression control in bacteria as well as in some plants and fungi.^[5] So far, RNA switches have been reported that bind specifically to essential coenzymes and vitamins, amino acids, glucosamine-6-phosphate, and the purine bases guanine and adenine. RNA switches are mostly found in the 5'-untranslated regions (5'-UTR) of messenger RNA (mRNA) and therefore belong to the noncoding part of the mRNA. Many RNA switches have a modular architecture: they consist of an aptamer domain or sensor region, which is responsible for ligand binding, and the so-called expression platform that transmits the ligand-binding state of the aptamer domain and thereby modulates gene expression. Ligand binding in the aptamer domain or sensor region leads to transcription termination, which abolishes ribosome binding or leads to different mRNA stabilities as a result of altered mRNA processing (Figure 1 and Table 1).

Sequence and secondary-structure analysis indicates that 2% of all genes in *B. subtilis* are regulated at least in part by a riboswitch mechanism. Binding of a small-molecule metabolite to the aptamer domain constitutes a direct feedback loop

[*] Prof. Dr. H. Schwalbe, J. Buck, B. Fürtig, J. Noeske
Institute for Organic Chemistry and Chemical Biology
Center for Biomolecular Magnetic Resonance
Johann Wolfgang Goethe-University Frankfurt
Max von Laue-Strasse 7, 60438 Frankfurt am Main (Germany)
Fax: (+49) 69-798-29515
E-mail: schwalbe@nmr.uni-frankfurt.de

Prof. Dr. J. Wöhnert
University of Texas Health Science Center SA
Department of Biochemistry
7703 Floyd Curl Drive, San Antonio, TX 78229 (USA)
Fax: (+001) 210-567-6595
E-mail: jewoe@biochem.uthscsa.edu



Supporting information for this article is available on the WWW under <http://www.angewandte.org> or from the author.

to either enhance or suppress the de novo synthesis of those proteins that are involved in the metabolic or catabolic pathway of the metabolite itself. The aptamer domains of naturally occurring riboswitches are in general significantly larger than their non-natural counterparts, even if they bind to similar ligands with an affinity in the low nanomolar range.

2. Riboswitches as Regulation Elements for Transcription and Translation

Riboswitches have been reported that regulate gene expression either at the level of transcription or translation. In addition, it has been proposed that riboswitch mechanisms are even used to regulate the processing of mRNA and thereby presumably alter cellular mRNA stability.

The adenine riboswitch from *V. vulnificus* has been proposed to regulate the *add* operon during translation as a so-called “on switch” (Figure 1a). As proposed by Patel and

co-workers, binding of adenine induces the formation of a helical element that releases the Shine–Dalgarno sequence (SD sequence) and the start codon.^[8b] The translation of the *add* operon is therefore up-regulated at high concentrations of adenine. We note, however, that the prediction of the secondary structure of this riboswitch also allows a conformation in which adenine is bound to the fully formed aptamer domain and the SD sequence is still masked by a helical rearrangement (see Supporting Information).

The thiamine pyrophosphate (TPP) riboswitch (Figure 1d) operates at the level of translation as well. In the absence of ligand, the SD sequence is single-stranded as a complementary anti-SD sequence is involved in long-range interactions with an anti-anti-SD sequence. Binding of the metabolite TPP releases the anti-SD that then pairs with the SD sequence. Therefore, in contrast to the adenine riboswitch from *V. vulnificus*, the TPP riboswitch acts as an “off switch”: high concentrations of metabolite down-regulate the translation of the *thiM* operon in *E. coli*. In addition, a TPP riboswitch was found in the 3'-untranslated region (3'-UTR) of the *thiC* operon from *A. thaliana* and is therefore proposed to operate on the level of mRNA stability instead of being involved in translational control as described for the *thiM* operon in *E. coli*.^[6]

The fascinating mechanisms of regulation can, however, be even more striking: The same adenine-sensing aptamer domain that regulates translation in *V. vulnificus* acts as a transcriptional “on switch” for the *ydhL* (now named *pbuE*) operon in *B. subtilis*. Aptamer domains are apparently designed as modules and used for transcriptional or for translational control depending on the nature of the expression platform. A single nucleotide mutation (U74C) dramat-



Harald Schwalbe, born in 1966, obtained his PhD with C. Griesinger from the University in Frankfurt in 1993. After a postdoctoral stay with C. M. Dobson (Oxford, UK), he completed his habilitation at the University of Frankfurt (1999) before joining the MIT (CA, USA) as an assistant professor. He was appointed Professor of Organic Chemistry at the University of Frankfurt in 2001. His research is focused on the determination of the structure, dynamics, and functions of proteins and RNA using high-resolution NMR spectroscopy.



Jens Wöhnert, born in 1970, studied biochemistry at the Martin Luther University, Halle/Saale, and completed his PhD at the Institute of Molecular Biotechnology, Jena, where he applied NMR spectroscopy to study the structure of RNA and RNA–protein complexes. In 2000, he joined the group of Prof. Schwalbe at the Francis Bitter Magnet Laboratory at MIT. In 2002, he was appointed director of the SFB 579 “RNA–Ligand Interactions” research group at the University of Frankfurt. Since 2005, he is an assistant professor at the University of Texas, San Antonio.



Boris Fürtig, born in 1978, studied biochemistry at the University of Frankfurt and completed his diploma research project in the group of Prof. Schwalbe in spring 2003. He is currently completing his PhD in the group of Prof. Schwalbe on the investigation of RNA by NMR spectroscopic methods.



Jonas Noeske, born in 1978, studied biochemistry at the University of Frankfurt and completed his diploma research project in the group of Prof. Schwalbe in spring 2004. He is currently working on his PhD in the group of Prof. Schwalbe, investigating riboswitches by NMR spectroscopy.



Janina Buck, born in 1980, studied chemistry at the University of Frankfurt and completed her diploma research project in the group of Prof. Schwalbe in spring 2005. She is currently working on her PhD in the group of Prof. Schwalbe, undertaking kinetic investigations of ligand-induced RNA folding by NMR spectroscopy.

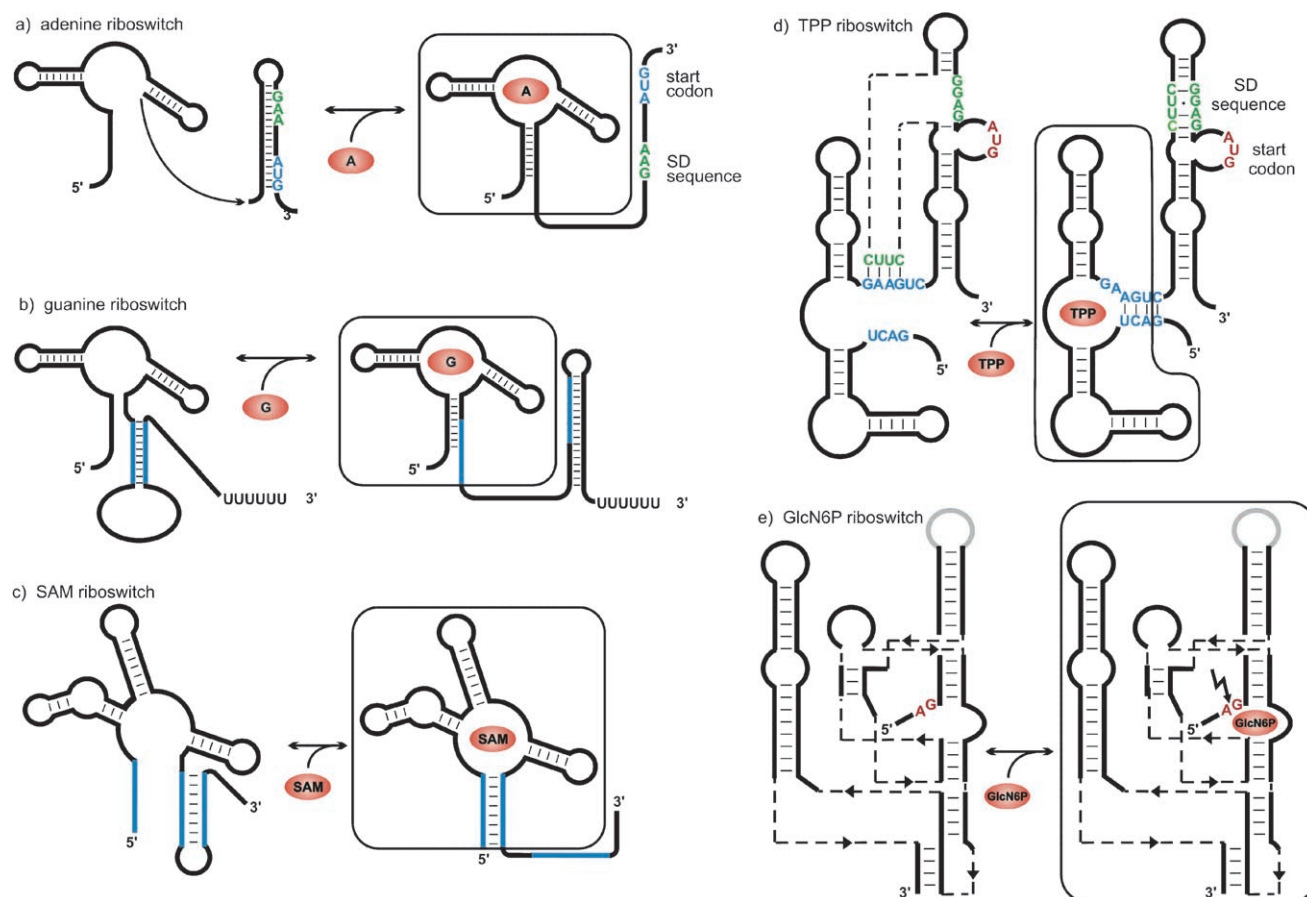


Figure 1. RNA switches, whose aptamer domains have been solved: a) adenine riboswitch from *V. vulnificus*, b) guanine riboswitch from *B. subtilis*, c) SAM riboswitch from *T. tengcongensis*, d) TPP riboswitch from *E. coli*, and e) *glmS* ribozyme from *T. tengcongensis*.

ically changes the affinity of the adenine riboswitch to bind to guanine/hypoxanthine (Figure 1b), but no longer bind to adenine as discussed below (Figure 2a,b).^[14] The guanine/hypoxanthine riboswitch regulates the *xpt-pbuX* operon in *B. subtilis* that codes for genes involved in the recycling of purine and the de novo biosynthesis of purine and acts as a transcriptional off switch.

A more indirect way of gene regulation may be involved for the *glmS* riboswitch which regulates the *glmS* gene in *B. subtilis*. The *glmS* riboswitch is a ribozyme in which gene regulation is not linked to conformational switching between alternating secondary structures. Rather, bond cleavage in the 5'-UTR of mRNA is observed when the ligand glucosamine-6-phosphate binds to the aptamer part. It is proposed that the in vitro enzymatic activity of the *glmS* riboswitch is the cellular regulation principle, as it would be in agreement with the in vivo observed down-regulation of gene expression.^[7]

3. Molecular Recognition of Ligands by RNA Switches

High-resolution structures are available for the complexes of the aptamer domains of the guanine/adenine-binding riboswitches,^[8] the TPP-binding riboswitches,^[9] the SAM-

binding riboswitch,^[10] and the *glmS* ribozyme^[11,12] (see Figure 1 and Table 1). Some of these structures have already been described in review articles.^[13]

The exact nature of the RNA–ligand interactions in the different complexes of RNA switches varies widely owing to the chemical diversity of the different ligands. Noncanonical structural elements such as base triples and base quadruples and non-Watson–Crick base pairs are utilized to form the ligand-binding pockets. The structures reveal a multitude of novel interaction possibilities that show how RNA can target small molecules. Therefore, beside the interest in revealing the regulation mechanisms of riboswitches, these structures are of great importance in designing novel small molecules that bind RNA with high affinities ($K_D < 100$ nM) and specificities.

Biophysical studies have revealed that the differences in the chemical structures of purine analogues have a great influence on the binding affinities of these ligands to purine riboswitches.^[5a,14] The X-ray crystal structures^[8a,b,d] and NMR studies^[8c] of the ligand-bound state of the purine riboswitches, notably the guanine and the adenine riboswitch, show the formation of a complex binding pocket, where almost all positions of the heterocyclic purine metabolite are recognized by the RNA (Figure 2a,b). For both riboswitches, the N3/N9 edge of the ligand is bound to uridine residue U51, the N7 of

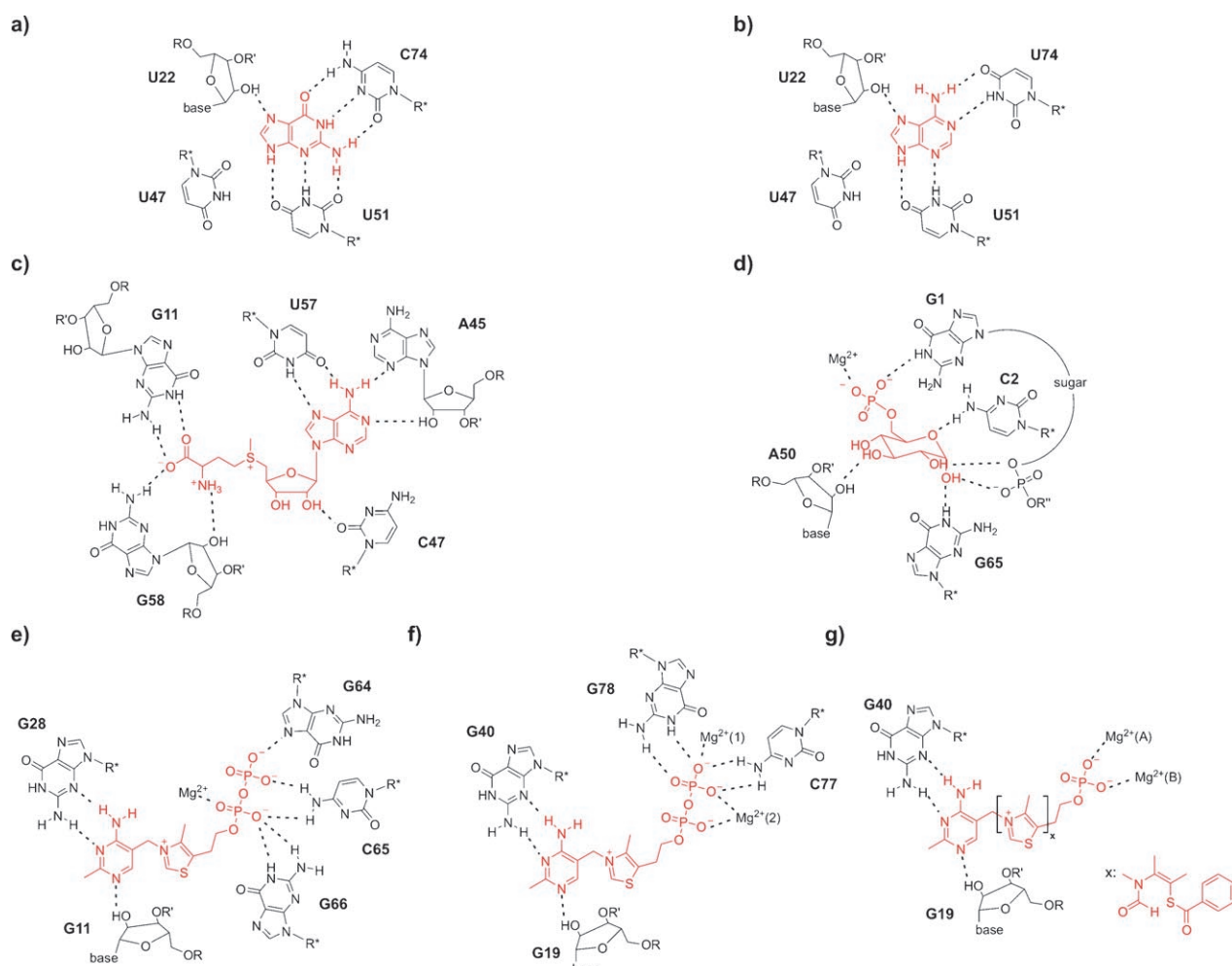


Figure 2. Molecular recognition of ligands (red) by RNA switches: a) guanine by the guanine riboswitch from *B. subtilis*, b) adenine by the adenine riboswitch from *B. subtilis*/*V. vulnificus*, c) SAM by the SAM riboswitch from *T. tengcongensis*, d) glucose-6-phosphate by the *glmS* ribozyme from *T. tengcongensis*, e) TPP by the TPP riboswitch from *A. thaliana*, f) TPP by the TPP riboswitch from *E. coli*, and g) TMP by the TPP riboswitch from *E. coli* (x: benfotiamine).

Table 1: Summary of X-ray crystal structures of solved aptamer domains of RNA switches.

RNA switch	Regulated gene	Ligand	Resolution [Å]	PDB accession code	Ref.
guanine	<i>xpt-pbuX</i> in <i>B. subtilis</i>	hypoxanthine	1.95	1U8D	[8a]
guanine	<i>xpt-pbuX</i> in <i>B. subtilis</i>	guanine	2.4	1Y27	[8b]
guanine C74U mutant	n.a.	2,6-diaminopurine	2.15	2B57	[8d]
adenine	<i>add</i> in <i>V. vulnificus</i>	adenine	2.1	1Y26	[8b]
thiamine pyrophosphate	<i>thiC</i> in <i>A. thaliana</i>	TPP	2.9	2CKY	[9a]
thiamine pyrophosphate	<i>thiM</i> in <i>E. coli</i>	TPP	2.05	2GDI	[9b]
S-adenosylmethionine	<i>metF-metH2</i> in <i>T. tengcongensis</i>	SAM	2.9	2GIS	[10]
thiamine pyrophosphate	<i>thiM</i> in <i>E. coli</i>	TPP	2.5	2HOJ ^[a]	[9c]
thiamine pyrophosphate	<i>thiM</i> in <i>E. coli</i>	TMP	2.89	2HOM	[9c]
thiamine pyrophosphate	<i>thiM</i> in <i>E. coli</i>	benfotiamine	3.0	2HOO	[9c]
thiamine pyrophosphate	<i>thiM</i> in <i>E. coli</i>	pyrithiamine	3.3	2HOP	[9c]
<i>glmS</i> ribozyme	<i>glmS</i> in <i>T. tengcongensis</i>	glucose-6-phosphate	2.10	2HO7 ^[a]	[12]

[a] See also: 2HOK and 2HOL. [b] See also: 2GCV, 2H0S, 2H0W, 2H0X, 2H0Z, 2H06, and 2GCS. n.a.: not applicable.

the Hoogsteen edge of the purines shows a hydrogen bond to the 2'-OH group of U22, and the X-ray crystal structures report to some extent^[8a,b] a hydrogen-bonding interaction of N9 to residue U47. The main difference in the two purine riboswitches is the nucleotide in the 74-position which allows

for a specific Watson-Crick base-pairing interaction of the ligand with the complementary nucleotide. In the case of the ligand guanine the nucleotide of the RNA is therefore a cytidine, while the ligand adenine is recognized by a uridine. Direct binding of the RNA to the N3/N9 edge of the purine

ligands discriminates the nucleobase against N9-glycosylated nucleosides and nucleotides which are also present in the cell.

Similarly, in the SAM riboswitch almost all functional groups of the ligand are involved in ligand recognition by the RNA (Figure 2c).^[15,10] The ligand SAM can structurally be divided into two subunits: an adenosyl moiety and a chain derived from methionine which carries a methylated, positively charged sulfur atom and the charged α -amino acid group attached to the 5'-end of the nucleoside. The compact conformation of the bound ligand can be pictured with the two subunits stacking on each other and therefore stabilizing this conformation through π -cation interactions. The adenine heterocycle is involved in the formation of a base triple with the flanking nucleobases A45 and U57. The 2'-OH sugar hydroxy group of the ligand is hydrogen-bonded to position O4 in residue C47. The oxygen atoms of the terminal carboxylate group show hydrogen-bonding interactions to the Watson-Crick site of residue G11 and to the exocyclic amino group of nucleotide G58; both nucleotides are part of the base triple G11·C44-G58. The positively charged, methylated sulfur atom is within about 4 Å distance of the O2 atoms of U7 and U88 and can therefore participate in electrostatic interactions. This interaction explains the approximately 100-fold higher K_D value of the ligand SAM compared to the neutral ligand S-adenosylhomocysteine (SAH), in which the sulfur atom is neither methylated nor positively charged. However, the methyl group bound to the sulfur atom is not directly recognized by the RNA, as seen in the crystal structure of the SAM riboswitch.^[11d] Interestingly, ligand binding to the RNA switch neither involves magnesium ions in the binding pocket to compensate the negatively charged carboxylate group of the ligand nor involves the phosphate backbone in direct interactions with the ligand to compensate the net charges of the positive functional groups of the ligand.

The crystal structure of the *glmS* ribozyme bound to glucose-6-phosphate (Glc6P)^[12] reveals the ligand-bound state of this catalytic riboswitch and gives insight into the catalytic activity. Despite its isosteric structure compared to the activating ligand glucosamine-6-phosphate (GlcN6P), Glc6P is a competitive inhibitor and therefore the RNA is still in its precleaved state in the presence of Glc6P (Figure 2d). The crystal structures of the ligand-free RNA and the RNA following cleavage yield information about the correlation of ligand binding and ribozyme function. The catalytic activation takes place in the binding pocket, which acts as the active site of the ribozyme, therefore ligand binding, ligand recognition, and ligand-induced activation are correlated.

Compared to other riboswitch structures, the ligand-binding pocket is rigid and preorganized^[16,12] and is not characterized through a complete embedding of the bound ligand but instead through a more open, solvent-accessible form. However, ligand recognition is specific and activation of the catalytic function is significant. The structure of the riboswitch-ligand complex provides an explanation for this observation because the entire ligand with its sugar moiety and phosphate group is involved in the interaction. Cleavage requires the presence of the amino group as in GlcN6P. Activation seems to require the correct orientation of the

functional group and its capacity to take part in a proposed acid-base reaction. This observation also explains the necessity of water molecules to be present in the active site during the cleavage process. Complexes with trapped ligands that lead to cleavage have not yet been reported.

Hydrogen-bonding interactions that stabilize the RNA-ligand complex are formed between Glc6P, which is bound as the α -anomer, and the unpaired nucleotide G1. The nucleotide G1 surrounds the ligand and binds to the phosphate and the sugar hydroxy groups. Furthermore, the ligand forms hydrogen bonds to C2, G65, and the 2'-OH group of A50. The negative charge of the phosphate group is compensated by the coordination of a magnesium ion, which lies approximately 10 Å from the scissile phosphate and is therefore not involved in catalysis. In addition, the 2'-OH group of the ligand forms a hydrogen bond to one water molecule found in the active site.

In contrast to many other riboswitches, not all functional groups of the biologically active metabolite TPP are recognized by the TPP riboswitch (Figure 2e-g). TPP itself can structurally be divided into a pyrimidine heterocycle, a thiazole ring, and a pyrophosphate moiety. As seen in all published crystal structures^[9a,b,c] of this riboswitch (see Table 1), the ligand moiety with the two heterocycles adopts an extended form whereas the pyrophosphate adopts a bent conformation. In the TPP-bound state, two helices are oriented in parallel fashion. The pyrimidine ring of the ligand binds to one helix, and the pyrophosphate end binds to the other helix. The pyrimidine ring and the phosphate moiety of the ligand are directly recognized, in contrast to the bridging thiazole ring, which is not directly bound and therefore can also be replaced by other elements (Figure 2g).^[9c,17] All reported crystal structures reveal the presence of magnesium ions in the pyrophosphate binding pocket, compensating the negatively charged phosphate groups, a finding that is in agreement with the biochemically and NMR spectroscopically observed strong magnesium dependence of ligand binding to the RNA.^[9d,17] The Watson-Crick site of the pyrimidine ring is found in all published structures to form hydrogen bonds with the sugar edge of a guanosine residue. In addition, one hydrogen bond is formed between position N1 of the ligand and a 2'-OH group of another guanosine nucleotide. The pyrophosphate binding pocket and the recognition of the pyrophosphate moiety differ in the various riboswitch elements derived from different organisms, and both depend on the bound ligand.

The structure of the TPP riboswitch from *A. thaliana* reported by Ban and co-workers^[9a] (Figure 2e) shows direct hydrogen bonds of G64, C65, and G66 to the pyrophosphate end of the ligand and further includes the participation of one magnesium ion in this binding pocket. The structure of the TPP riboswitch from *E. coli* published by Patel and co-workers^[9b] (Figure 2f) shows a different bonding scheme in the pyrophosphate binding pocket. Here, the phosphate groups are coordinated by two magnesium ions and furthermore form hydrogen bonds to the residues C77 and G78. Edwards et al.^[9c] reported that besides the magnesium-mediated contacts a hydrogen bond between G78 and a nonbridging oxygen atom of the terminal phosphate is the only direct contact from the ligand to the pyrophosphate

binding pocket. The crystal structure of the riboswitch complex with thiamine monophosphate (TMP)^[9c] shows in general the same hydrogen-bonding pattern as that with TPP (Figure 2g). In contrast to the TPP-bound RNA, there is no hydrogen bond between the ligand and nucleotide G78 in TMP-bound RNA. In the TPP-bound structure, one magnesium ion binds to both phosphate groups and, in addition, a second magnesium ion binds to the terminal phosphate group. In the TMP-bound structure, two magnesium ions bind to the only (terminal) phosphate group. Replacement of the ligand TMP with benfotiamine (BTP)^[9c] in which the central heterocycle is not a thiazole (Figure 2g with inset x), does not change the ligand-recognition mode compared to the TMP–RNA complex. Moreover, the crystal structure of the riboswitch complex with the ligand pyrithiamine (PT)^[9c] was reported (structure not shown). Although the pyrimidine part of the ligand does not change, no hydrogen bonds could be observed between the guanosine nucleotide (G40) and the ligand. Instead, the only direct contact between the RNA and the ligand is the hydrogen bond between N1 of PT and the 2'-OH group of a guanosine residue (G19), an interaction already described for all other ligands.

4. Secondary and Tertiary Interactions That Stabilize the Aptamer Domains of RNA Switches

In contrast to the smaller SELEX-derived aptamers, the structures of RNA switches also reveal numerous long-range RNA–RNA tertiary interactions, such as pseudoknots, that are not involved in the formation of the ligand-binding pocket but instead stabilize the global fold of the RNA structure. The folds of the aptamer domains of the riboswitches determined thus far are very compact owing to an extensive packing of the helical elements. This packing is facilitated by known motifs, for example, type I/II A-minor triple motifs, as well as newly observed structural elements, such as the base quadruples in the purine-binding riboswitches.^[18]

On the basis of the aptamer domain architecture, we can classify the riboswitch structures into two general types:

- Type I riboswitches reveal a three-way junction as the primary global architecture of their aptamer domains; members of type I include the purine-binding riboswitches, TPP-binding riboswitches, and the *glmS* ribozyme.
- Type II riboswitches include motifs where the aptamer domain is arranged in a four-way junction architecture; the structure of the SAM-I-binding riboswitch is a representative example.

4.1. Type I RNA Switches

The aptamer domains of the purine riboswitches bound to the respective ligand show a fundamental three-way junction architecture in which two parallel helices P2 and P3 are tightly packed together by a series of interconnecting hydrogen bonds between the apical loops L2 and L3 (Figure 3a,b). These hydrogen bonds span two base quadruples composed in

each case of a G–C Watson–Crick base pair and a non-canonical A·A or A·U base pair that interacts from the minor-groove side. The juxtaposition of the negatively charged RNA backbone regions which results in unfavorable electrostatic interactions is compensated by the binding of positively charged cations. The purine-binding pocket is located in the three-way junction element where base triples above (water-mediated base triple U22–A52·A73 and base triple A23·G46–C53) and below (base triple U20–A76·U49 and base triple A21–U75–C50) flank the ligand and form a nearly closed envelope. Binding of the ligand is critically dependent on the formation of the tertiary architecture, as revealed by the mutation introducing a tetraloop (four-nucleotide loop) as capping motif for the parallel-packed helices. This mutation renders the riboswitch incapable of ligand binding. NMR studies show that the loop–loop interaction is preorganized even in the absence of ligand.^[18]

A similar three-way junction architecture is observed for the TPP riboswitches (Figure 3c). Here, two helical elements are arranged in a parallel manner. In contrast to the purine riboswitches, the interacting helical elements are not made up of continuous helices but in each case of two helical arms that are connected by junction elements (P2/P3 with J2/3, and P4/P5 with J4/5). While ligand binding in the purine riboswitches is facilitated by the junction element of the central three-way junction, binding of TPP and its analogues involves the junction element J4/5 as a sensing element for the pyrophosphate and J2/3 as a sensing element for the pyrimidine moiety. Binding of TPP is one of the interactions to bridge the helical arms and shapes the whole molecule into its signaling form. Furthermore, this architecture is facilitated by a helix–loop interaction between helix P3 and loop L5 that is stabilized by monovalent cations.

The structure of the *glmS* ribozyme belongs to type I riboswitches with a three-way junction element. In this case, however, the three-way junction is not the major determinant of the tertiary structure of this riboswitch. The overall structure of this RNA molecule is dominated by three coaxial stacks of helices that are arranged side by side. Two helical elements, one consisting of helices P1, P2.2, P2, P3, and P3.1 (≈ 100 Å) and the other consisting of P4 and P4.1, surround the shorter central helical stack P2.1. The ribozyme is therefore a highly anisotropic molecule. The central feature of the structure is the double-pseudoknot core of the ribozyme that allows the positioning of the scissile phosphate group located at the 5'-end of helix P2.2 into the major groove of helix P2.1. To accomplish such a double-pseudoknot arrangement of the helices P2.1 and P2.2, four nonhelical crossovers are needed and are facilitated by a number of noncanonical interactions. The upper two crossovers have been classified as the roof of the active site by Klein et al.^[12] They are part of two conserved base triples (G34·G7–C30 and A35·C36–G53) that are the branch points for the three-way junction between P1, P2.2, and P2.1. Interestingly, on the floor side of the active site, two nucleotides are threaded through the loop between P2 and P2.1 and then stack onto the nucleotides of either one of the lower crossovers. Whereas in the lower part of the molecule a canonical pseudoknot comprising helices P3 and P3.1 can be found that stacks onto

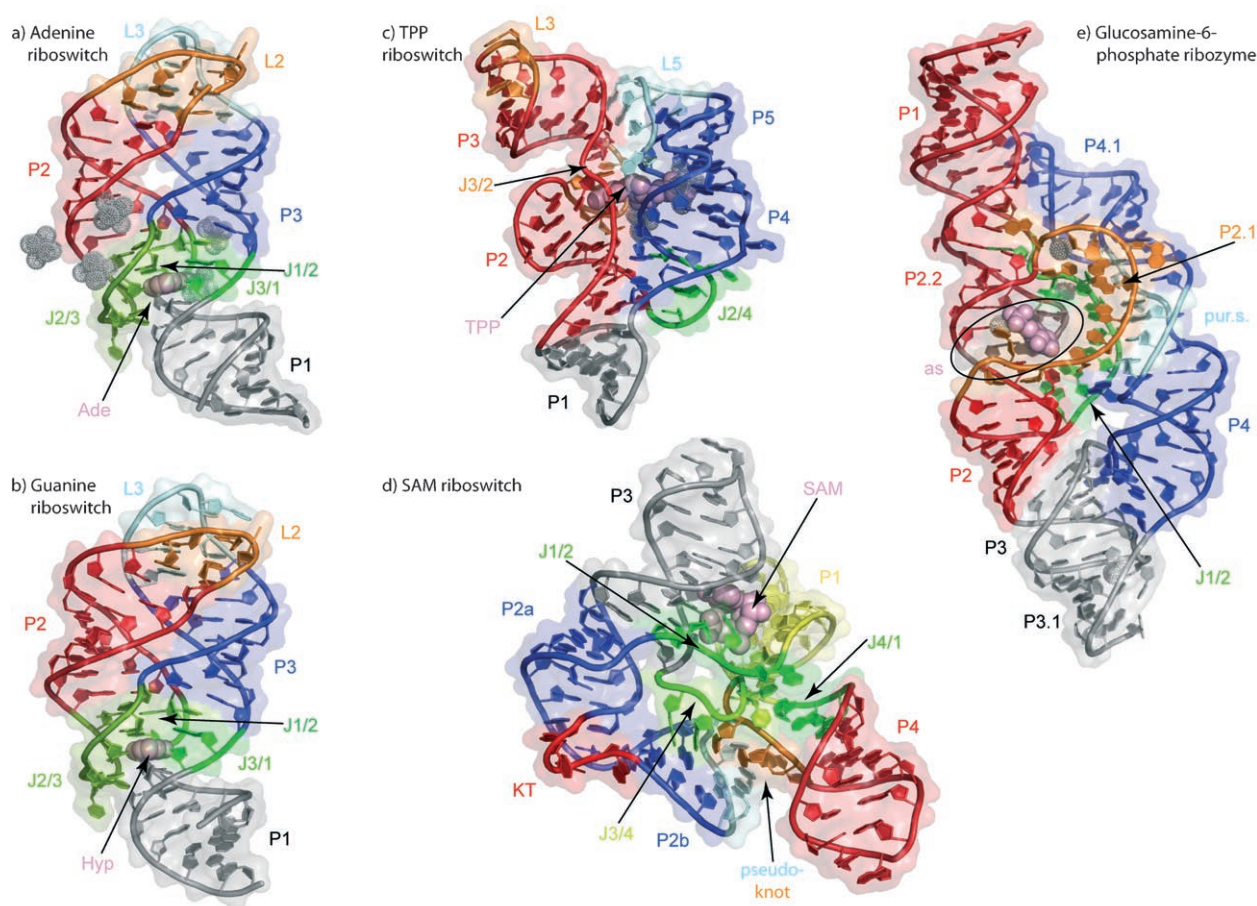


Figure 3. Three-dimensional structures of the aptamer domains of RNA switches (all RNA structures are shown as ribbon representations, ligands are shown in sphere representations and colored pale violet, and the surface is lightly shaded): a) complex of adenine riboswitch from *V. vulnificus* with adenine (pdb accession code: 1Y26), b) complex of guanine riboswitch from *B. subtilis* with hypoxanthine (1U8D), c) complex of TPP riboswitch from *E. coli* with TPP (2GDI), d) complex of SAM riboswitch from *T. tengcongensis* with SAM (2GIS), and e) complex of *glmS* ribozyme (before cleavage) from *T. tengcongensis* with Glc6P (2HO7). Structural elements are color coded (see text); the numbering follows the nomenclature given in the original publications; P: helices; J: junctional elements; L: loops; KT: kink turns; as: active side; pur.s.: purine stretch.

P2, the helices P4 and P4.1 form a coaxial stack that is a scaffolding element and acts as an abutment for P2.1. The positioning of this scaffold is maintained by several tertiary interactions: an A-minor interaction between A117 of the tetraloop L4.1 and C10–G31 of P1, and a six-purine stack consisting of A129/G128/A127/A104/A105/A106 that is formed by the internal loop between P4 and P4.1, enclosed in the minor groove of P2.1. As indicated by the low all-atom RMSD difference in the pre- and postcleavage state of the RNA molecule, the *glmS* ribozyme does not undergo a major conformational switching event upon ligand binding but just the cleavage of the scissile phosphodiester bond, and is therefore different in the mode of action to the other riboswitches described here.

4.2. Type II RNA Switches

In contrast to the riboswitch structures described so far, the SAM riboswitch has a four-way junction as its central structural element (Figure 3d). Around this four-way junction, stems and stem-loop structures are found. Two sets of

coaxially stacked helices are found: P2a and P3 as well as P1 and P4 with the intervening junction element J4/1. These two stacks are held together by the pairing of residue A85 in J4/1 with U64 in J3/4 and A24 in L2. This architecture holds the two stacks at an angle of 70° which results in a binding pocket for SAM that sits in the minor grooves of P1 and P3.

Two ligand-independent tertiary structure motifs should be mentioned that are necessary for the global architecture. On such motif is a kink-turn motif, which connects the helices P2a and P2b. This kink enables the formation of a pseudoknot structure by the pairing of L2 and J3/4. The structure of the pseudoknot is further stabilized by base triples between residues A85–U64–A24 which reside in P1 and P4, and by interaction of residues from J3/4 and P2b that form adenine-mediated base triples.

5. Open Questions Regarding the Regulation Mechanisms of RNA Switches

Biophysical studies pose challenges to a simple allosteric model of conformational switching to explain translational or

transcriptional regulation. According to this model, ligand binding to the aptamer domain would induce structural transitions in the secondary structure elements of the mRNA and release or mask regulation elements involved in transcription as well as translation (see Figure 1). However, as revealed by stopped-flow fluorescence studies^[19,8d] and by time-resolved NMR spectroscopy^[20] for the purine riboswitches and the FMN riboswitch, the rate constants at physiological ligand concentrations are too slow for a model in which ligand binding precedes the conformational switch and thereby regulates gene expression. Rather, the mechanism has to consider that the gene regulation is exerted during transcription and general protein transcription termination factors may also be important. In light of these comments, we would like to conclude this review article with a quote from Nudler:^[13b] "Therefore, to fully understand riboswitch functioning, the atomic resolution picture of ligand–RNA contacts needs to be put in the context of the whole expression platform, its folding process, and kinetic coupling dictated by the RNA polymerase."

The work was supported by the DFG (SFB 579: "RNA–Ligand Interaction"), the Fonds der Chemischen Industrie (predoctoral fellowship to J.N.), the Studienstiftung des Deutschen Volkes (predoctoral fellowship to B.F.), and the state of Hesse (Center for Biomolecular Magnetic Resonance (BMRZ)).

Received: October 10, 2006

Revised: November 13, 2006

Published online: January 17, 2007

- [1] a) A. D. Ellington, J. W. Szostak, *Nature* **1990**, *346*, 818–822; b) S. J. Klug, M. Famulok, *Mol. Biol. Rep.* **1994**, *20*, 97–107; c) J. Joyce, *Curr. Opin. Struct. Biol.* **1994**, *4*, 331–336.
- [2] a) M. Famulok, *Curr. Opin. Struct. Biol.* **1999**, *9*, 324–329, and references therein; b) T. Hermann, D. J. Patel, *Science* **2000**, *287*, 820–825.
- [3] D. H. Burke, L. Gold, *Nucleic Acids Res.* **1997**, *25*, 2020–2024.
- [4] a) J. Miranda-Rios, M. Navarro, M. Soberon, *Proc. Natl. Acad. Sci. USA* **2001**, *98*, 9736–9741; see also: G. D. Stormo, Y. Ji, *Proc. Natl. Acad. Sci. USA* **2001**, *98*, 9465–9467; b) W. Winkler, A. Nahvi, R. R. Breaker, *Nature* **2002**, *419*, 952–956; c) A. Mironov, I. Gusarov, R. Rafikov, L. Lopez, K. Shatalin, R. Kreneva, D. Perumov, E. Nudler, *Cell* **2002**, *111*, 747–756; d) S. D. Gilbert, R. T. Batey, *Cell. Mol. Life Sci.* **2005**, *62*, 2401–2404.
- [5] a) M. Mandal, B. Boese, J. E. Barrick, W. C. Winkler, R. R. Breaker, *Cell* **2003**, *113*, 577–586; b) N. Sudarsan, J. E. Barrick, R. R. Breaker, *RNA* **2003**, *9*, 644–647; c) T. Kubodera, M. Watanabe, K. Yoshiuchi, N. Yamashita, A. Nishimura, S. Nakai, K. Gomi, H. Hanamoto, *FEBS Lett.* **2003**, *555*, 516–520.
- [6] N. Sudarsan, J. E. Barrick, R. R. Breaker, *RNA* **2003**, *9*, 644–647.
- [7] W. C. Winkler, A. Nahvi, A. Roth, J. A. Collins, R. R. Breaker, *Nature* **2004**, *428*, 281–286.
- [8] a) R. T. Batey, S. D. Gilbert, R. K. Montange, *Nature* **2004**, *432*, 411–415; b) A. Serganov, Y. R. Yuan, O. Pikovskaya, A. Polonskaia, L. Malinina, A. T. Phan, C. Hobartner, R. Micura, R. R. Breaker, D. J. Patel, *Chem. Biol.* **2004**, *11*, 1729–1741; c) J. Noeske, C. Richter, M. A. Grundl, H. R. Nasiri, H. Schwalbe, J. Wöhnert, *Proc. Natl. Acad. Sci. USA* **2005**, *102*, 1372–1377; d) S. D. Gilbert, C. D. Stoddard, S. J. Wise, R. T. Batey, *J. Mol. Biol.* **2006**, *359*, 754–768.
- [9] a) S. Thore, M. Leibundgut, N. Ban, *Science* **2006**, *312*, 1208–1211; b) A. Serganov, A. Polonskaia, A. T. Phan, R. R. Breaker, D. J. Patel, *Nature* **2006**, *441*, 1167–1171; c) T. E. Edwards, A. R. Ferre-D'Amare, *Structure* **2006**, *14*, 1459–1468; d) J. Noeske, C. Richter, E. Stinhal, H. Schwalbe, J. Wöhnert, *ChemBioChem* **2006**, *7*, 1451–1456.
- [10] R. K. Montange, R. T. Batey, *Nature* **2006**, *441*, 1172–1175.
- [11] a) J. E. Barrick, K. A. Corbino, W. C. Winkler, A. Nahvi, M. Mandal, J. Collins, M. Lee, A. Roth, N. Sudarsan, I. Jona, J. K. Wickiser, R. R. Breaker, *Proc. Natl. Acad. Sci. USA* **2004**, *101*, 6421–6426; b) G. Mayer, M. Famulok, *ChemBioChem* **2006**, *7*, 602–604; c) J. A. Jansen, T. J. McCarthy, G. A. Soukup, J. K. Soukup, *Nat. Struct. Mol. Biol.* **2006**, *13*, 517–523; d) J. Lim, W. C. Winkler, S. Nakamura, V. Scott, R. R. Breaker, *Angew. Chem.* **2006**, *118*, 978–982; *Angew. Chem. Int. Ed.* **2006**, *45*, 964–968.
- [12] D. J. Klein, A. R. Ferre-D'Amare, *Science* **2006**, *313*, 1752–1756.
- [13] a) S. Reichow, G. Varani, *Nature* **2006**, *441*, 1054–1055; b) E. Nudler, *Cell* **2006**, *126*, 19–22; c) S. D. Gilbert, R. T. Batey, *Chem. Biol.* **2006**, *13*, 805–807.
- [14] M. Mandal, R. R. Breaker, *Nat. Struct. Mol. Biol.* **2004**, *11*, 29–35.
- [15] W. C. Winkler, A. Nahvi, N. Sudarsan, J. E. Barrick, R. R. Breaker, *Nat. Struct. Biol.* **2003**, *10*, 701–707.
- [16] K. J. Hampel, M. M. Tinsley, *Biochemistry* **2006**, *45*, 7861–7871.
- [17] T. Yamauchi, D. Miyoshi, T. Kubodera, A. Nishimura, S. Nakai, N. Sugimoto, *FEBS Lett.* **2005**, *579*, 2583–2589.
- [18] J. Noeske, J. Buck, B. Fürtig, H. Nasiri, H. Schwalbe, J. Wöhnert, *Nucleic Acids Res.* **2007**, in press.
- [19] a) J. K. Wickiser, W. C. Winkler, R. R. Breaker, D. M. Crothers, *Mol. Cell* **2005**, *18*, 49–60; b) J. K. Wickiser, M. T. Cheah, R. R. Breaker, D. M. Crothers, *Biochemistry* **2005**, *44*, 13404–13414.
- [20] a) J. Buck, B. Fürtig, J. Noeske, J. Wöhnert, H. Schwalbe, unpublished results; b) J. Buck, diploma thesis, Frankfurt, **2005**.